

AD-780 247

CESIUM DIDEUTERIUM ARSENATE CRYSTAL  
DEVELOPMENT

Joseph F. Balascio, et al

Isomet Corporation

Prepared for:

Office of Naval Research

20 April 1974

DISTRIBUTED BY:

**NTIS**

National Technical Information Service  
U. S. DEPARTMENT OF COMMERCE  
5285 Port Royal Road, Springfield Va. 22151

UNCLASSIFIED

Security Classification

AD-780247

## DOCUMENT CONTROL DATA - R &amp; D

(Security classification of title, body of abstract and indexing annotation must be entered when the overall report is classified)

## 1. ORIGINATING ACTIVITY (Corporate author)

Isomet Corporation  
103 Bauer Drive  
Oakland, New Jersey 07436

## 2a. REPORT SECURITY CLASSIFICATION

Unclassified

## 2b. GROUP

## 3. REPORT TITLE

CESIUM DIDEUTERIUM ARSENATE CRYSTAL DEVELOPMENT

## 4. DESCRIPTIVE NOTES (Type of report and inclusive dates)

Final Technical Report (period covered by this report 3/1/73 - 3/31/74)

## 5. AUTHOR(S) (First name, middle initial, last name)

Joseph F. Balascio  
Gabriel M. Loiacono

## 6. REPORT DATE

20 April 1974

## 7a. TOTAL NO. OF PAGES

71

## 7b. NO. OF REFS

34

## 8a. CONTRACT OR GRANT NO.

N00014-73-C-0372

## b. PROJECT NO.

ARPA Order No. 2364

## c.

Program Code 3D10

## d.

## 9a. ORIGINATOR'S REPORT NUMBER(S)

TR: 134

## 9b. OTHER REPORT NO(S) (Any other numbers that may be assigned this report)

## 10. DISTRIBUTION STATEMENT

## 11. SUPPLEMENTARY NOTES

## 12. SPONSORING MILITARY ACTIVITY

Office of Naval Research

## 13. ABSTRACT

The results on the growth of cesium dideuterium arsenate from aqueous and mixed solvent systems are reported. Particular emphasis had been placed on the analyses of the factors affecting the solution chemistry of CD\*A and their affect upon the resultant growth. The phase stability, solubility and supersaturation of CD\*A were determined in both solvent systems. Actual deuteration levels in the crystal and aqueous growth solution are reported and discussed.

Preliminary data show the mixed solvent system to be very promising for the reproducible growth of high optical quality CD\*A.

Reproduced by  
NATIONAL TECHNICAL  
INFORMATION SERVICE  
U S Department of Commerce  
Springfield VA 22151

DD FORM 1473  
1 NOV 65

Security Classification

14

KEY WORDS	LINK A		LINK B		LINK C	
	ROLE	WT	ROLE	WT	ROLE	WT
Cesium Dideuterium Arsenate crystallographic Data phase stability solubility growth data deuteration level						

**ISOMET**

TR: 134  
JOB: 5261

CESIUM DIDEUTERIUM ARSENATE CRYSTAL DEVELOPMENT

Final Technical Report  
April 20, 1974

Sponsored by  
Advanced Research Projects Agency  
ARPA Order No. 2364

under

Contract No. N00014-73-C-0372

Scientific Officer: Director, Physics Program  
Physical Sciences Division  
Office of Naval Research  
Department of Navy  
800 North Quincy Street  
Arlington, Virginia 22217



Program Code No. 3D10  
Amount of Contract: \$97,926  
Effective Date of Contract: March 1, 1973  
Contract Expiration Date: March 31, 1974  
Principal Investigators: J.F. Balascio and G.M. Loiacono  
Phone No. (201) 337-3811  
Authors: J.F. Balascio and G.M. Loiacono

The views and conclusions contained in this document are those of the authors and should not be interpreted as necessarily representing the official policies, either expressed or implied, of the Advanced Research Projects Agency or the U.S. Government.

*il*



TABLE OF CONTENTS

	<u>PAGE</u>
ABSTRACT.....	i
SUMMARY.....	ii
1. INTRODUCTION.....	1
2. PHYSICAL AND CHEMICAL PROPERTIES OF $\text{CsD}_2\text{AsO}_4$ ...	3
2.1 Crystallographic Data.....	3
2.2 Preparation of $\text{CsD}_2\text{AsO}_4$ .....	6
3. THE $\text{CsD}_2\text{AsO}_4$ - $\text{D}_2\text{O}$ SYSTEM.....	10
3.1 Phase Stability of $\text{CsD}_2\text{AsO}_4$ .....	13
3.2 Solubility of $\text{CsD}_2\text{AsO}_4$ in $\text{D}_2\text{O}$ .....	16
3.3 Specific Gravity and Kinematic Viscosities of CD*A Solutions.....	17
3.4 Supersolubility of $\text{CsD}_2\text{AsO}_4$ in $\text{D}_2\text{O}$ .....	23
4. THE $\text{CsD}_2\text{AsO}_4$ - $\text{D}_2\text{O}$ - $\text{R(OD)}_n$ SYSTEM.....	29
4.1 Phase Stability of $\text{CsD}_2\text{AsO}_4$ .....	30
4.2 Solubility of $\text{CsD}_2\text{AsO}_4$ in $\text{D}_2\text{O}$ - Glycol.....	30
4.3 Supersolubility of $\text{CsD}_2\text{AsO}_4$ in $\text{D}_2\text{O}$ - Glyco'	32
5. GROWTH AND CHARACTERIZATION OF SINGLE CRYSTAL $\text{CsD}_2\text{AsO}_4$ .....	34
5.1 Seed Preparation.....	34
5.2 Aqueous Growth Data.....	35
5.3 Mixed Solvent Growth Data.....	47
5.4 The Actual Deuteration Level in $\text{Cs(D}_{1-x}\text{H}_x)_2\text{AsO}_4$ Crystals.....	50

TABLE OF CONTENTS (CONTINUED)

	<u>PAGE</u>
5.5 Optical Transmission.....	53
5.6 Thermal Stability of CD*A.....	53
6. CONCLUSIONS.....	57
7. RECOMMENDATIONS.....	59
8. REFERENCES.....	61

SUMMARY

This is the Final Technical Report of a research program supported by The Advanced Research Projects Agency of the Department of Defense and monitored by ONR under Contract NO0014-73-C-0372.

Under this contract, the solution chemistry of cesium dideuterium arsenate in heavy water was completely determined. To a limited extent, the solution chemistry of CD\*A in D<sub>2</sub>O - deuterated glycol was also determined. Through the course of this investigation, the solution and growth parameters were found to have a profound effect upon the resultant growth of CD\*A.

Cesium dideuterium arsenate was determined to be the primary crystalline phase in the P<sub>H</sub> range of 3.0 to 9.0 over the temperature range of 60 to 10°C in D<sub>2</sub>O. In the 70%D<sub>2</sub>O - 30%D glycol system, CD\*A was the primary crystalline phase over the P<sub>H</sub> interval of 4.0 to 6.0 in the temperature range of 45 to 20°C. The saturation concentration was experimentally determined and the supersaturation calculated in both solvent systems as a function of temperature. It was determined that both the saturation and supersaturation concentrations of CD\*A were reduced by more than a factor of two at any particular temperature in the mixed solvent system.

The growth problems encountered in aqueous solution growth of CD\*A were flanging, tapering along the Z direction, edge and corner growth, multiple growth and irregular changes



## ISOMET

in the solubility as a function of temperature  $\left[ \left( \partial s / \partial T \right)_{n_i, P} \right]$ . These growth problems were determined to be a function of the saturation concentration,  $P_H$  and seed preparation techniques. Although relatively large pieces of CD\*A single crystals (1 inch cube) were successfully grown, it was determined that, under the best possible growth conditions, the reproducible growth of CD\*A could not be accomplished in  $D_2O$ . Through the course of this investigation, it was found that the average actual deuteration level in a CD\*A crystal grown from aqueous solutions was  $85.62 \pm 0.05$  mole % D and that of the growth solution was  $92.99 \pm 0.05$  mole % D. Compared to the published data on CD\*A, this represents the highest deuteration level ever reported.

It was also determined that most of the growth defects and problems associated with the aqueous growth of CD\*A were eliminated or controllable in the mixed solvent system. Though preliminary, these data show the mixed solvent system to be very promising for the reproducible growth of high optical quality CD\*A.



## 1. INTRODUCTION

There is a need for high average laser power at 0.53 microns in the form of short pulses generated at a high repetition rate. This particular wavelength is desirable for undersea systems because of the high optical transmission of seawater at this wavelength.

Recent experimental work has demonstrated that CD\*A is the most promising non-linear material for this particular SHG application. It has been reported that this material possesses the best overall efficiency, resistance to laser damage and thermal failure of all the non-linear materials tested.<sup>1</sup> Besides its high damage threshold, CD\*A has a large angular acceptance ( $\Delta T_{1/2} = 5.6^{\circ}\text{C}$ ) for temperature phase-matching.

Although these reported data on CD\*A show great promise, the optimization of CD\*A as a SHG material has not been accomplished. The SHG evaluation data heretofore reported on commercially available CD\*A has not been correlated with

- i) the actual deuteration in the crystal.
- ii) the absorptivity at 1.06  $\mu\text{m}$
- iii) the optical perfection (refractive index homogeneity) of the single crystals.

The main reason for this lack of correlation has been the non-reproducibility of the growth of CD\*A single crystals.

The objective of this program was the reproducible growth of cesium dideuterium arsenate single crystals of the highest deuteration level possible. To achieve this goal,

particular emphasis had been placed on the analysis of the factors affecting the solution chemistry of CD\*A. Through the course of this systematic investigation, the following variables were found to have a profound effect upon the growth of cesium dideuterium arsenate:

- i) The purity of initial reagents
- ii) The saturation temperature of the solution
- iii) The supersaturation concentration
- iv) The  $P_H$  of the solution
- v) The seed orientation
- vi) The seed surface preparation
- vii) The rotation speed
- viii) The solvent system
- ix) The deuteration level.

These factors not only affected the perfection of the cesium dideuterium arsenate single crystals, but also, the growth rates along particular crystallographic directions.

## 2. PHYSICAL AND CHEMICAL PROPERTIES OF $\text{CsD}_2\text{AsO}_4$

### 2.1 Crystallographic Data

Cesium dideuterium arsenate and its hydrogen analog belong to space group  $I \bar{4}2d$  and have tetramolecular unit cells. Other crystals which belong to this space group are KDP,  $\text{KD}^*\text{P}$ , ADP,  $\text{AD}^*\text{P}$ , KDA, and RDP.

Heretofore, no data had been published on the lattice constants or the powder diffraction pattern of cesium dideuterium arsenate. However, there are two sets of conflicting data published on the lattice constants of cesium dihydrogen arsenate (CDA).<sup>2-3</sup> The powder diffraction data reported by these authors are essentially the same but, the (h k l) assignments differed thereby resulting in different axial lengths. Table 1 is a compilation of these crystallographic data.

It is known that the substitution of deuterium for hydrogen in this type of compound changes the axial lengths by only slight amounts (0.01 to 0.06 Å).<sup>4</sup> Therefore, determining the axial lengths of  $\text{CD}^*\text{A}$  by accurately indexing its powder diffraction pattern, would result in the confirmation of the best set of published values for the lattice constants of CDA.

Precision powder diffraction data were obtained on  $\text{CsD}_2\text{AsO}_4$  at one-eighth of a degree  $2\theta$  per minute with a chart speed of 5 cm/min. Nickel filtered  $\text{CuK}\alpha$  radiation was used. Linde  $\text{Al}_2\text{O}_3$  (0.3  $\mu$ ) powder was employed as an external calibration standard. Table 2 contains the powder diffraction data obtained

TABLE 1

Comparison of Published Lattice Constants For  $\text{CsH}_2\text{AsO}_4$

Ferrari et. al. (2)

Shklovskaya et. al. (3)

$a_o$  ( $\text{\AA}$ ) 7.98

7.94

$c_o$  ( $\text{\AA}$ ) 7.87

7.70

$D_x$  (g/cc) 3.62

3.73

TABLE 2

Powder Diffraction Data For Cesium D-deuterium Arsenate

$$a_o = 7.963 \pm .008 \text{ \AA} \quad c_o = 7.887 \pm 0.008 \text{ \AA}$$

$$D_x = 3.65 \text{ g/cc}$$

$\frac{d}{\text{\AA}}$	$\frac{I}{I_o}$	(h k l)
3.98	85	200
3.22	100	112
2.81	36	220
2.52	4	310
2.50	3	103
2.122	58	312
1.992	4	400
1.782	13	420
1.766	14	204
1.696	13	332
1.615	10	224

on CD\*A. The axial lengths of CD\*A and CDA are compared with other deuterated and non-deuterated isomorphs in Table 3. The data in Tables 2 and 3 reveal that Ferrari et. al. data on CDA are the more accurate and that CD\*A is most similar to AD\*P with respect to published values of the direction and magnitude of axial length changes upon deuteration.

## 2.2 Preparation of Cesium Dideuterium Arsenate

Table 4 lists the sources and relative purities of the reagents employed to synthesize  $\text{CsD}_2\text{AsO}_4$ .

Two cesium salts were initially employed for this synthesis:  $\text{Cs}_x\text{O}_y$  ( $\text{Cs}_2\text{O}$  plus sub- and superoxides of cesium) and anhydrous  $\text{Cs}_2\text{CO}_3$ . Aqueous solutions of these salts were prepared and filtered (hot) through a  $0.6 \mu$  teflon millipore filtration system. Of these two, the  $\text{Cs}_2\text{CO}_3$  solution was the better one to employ from the standpoints of stoichiometry and ease of handling. No differences were detected in the CD\*A prepared from either reagent.

The preparation of aqueous solutions of  $\text{D}_3\text{AsO}_4$  were done in the same manner as the cesium salt solutions. Great care was taken to use only slight excesses of  $\text{D}_2\text{O}(l)$  above that required for stoichiometry. "Gettered" high purity nitrogen flushes were employed during preparation in order to minimize  $\text{D} \leftrightarrow \text{H}$  exchanges with the atmosphere. The basic reaction for the synthesis is

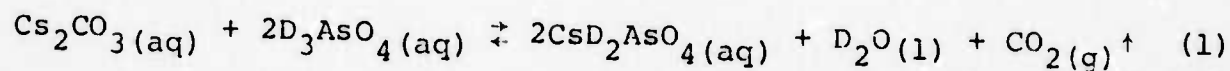


TABLE 3

Axial Lengths of Various  
Alkali Phosphate and Arsenate Crystals

<u>Material</u>	<u>a<sub>0</sub><sup>0</sup> (Å)</u>	<u>c<sub>0</sub><sup>0</sup> (Å)</u>
CD*A	7.963	7.887
KD*A	7.640	7.162
AD*P	7.499	7.548
KD*P	7.468	6.930
CDA	7.98	7.87
KDA	7.624	7.162
ADP	7.510	7.564
KDP	7.448	6.977



TABLE 4

Reagents Employed For The Synthesis  
Of Cesium Dideuterium Arsenate

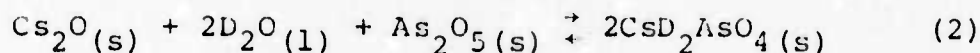
<u>Reagent</u>	<u>Purity</u>	<u>Vendor</u>
$\text{Cs}_2\text{CO}_3$	99.94%	Kawecki Berylco Industries, Inc.
$\text{Cs}_2\text{CO}_3$	99.99 <sup>+</sup> %	Apache Chemicals, Inc.
$\text{Cs}_2\text{O}$	99.90%	Cerac/Pure, Inc.
$\text{As}_2\text{O}_5$	99.999%	Rocky Mountain Research, Inc.
$\text{As}_2\text{O}_5$	99.999%	Cerac/Pure, Inc.
$\text{As}_2\text{O}_5$	99.3%	J.T. Baker Chemical Company
$\text{D}_2\text{O}$	99.80%	U.S. Atomic Energy Commission

## ISOMET

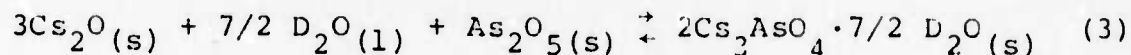
To prepare crystalline CD\*A, solutions of the two reagents saturated at high temperatures were slowly mixed together and then the solution slowly cooled to room temperature. Vacuum distillation was employed to remove further amounts of CD\*A from a solution. All crystalline CD\*A, employed for saturation point adjustment, was recrystallized at least twice.

### 3. THE $\text{CsD}_2\text{AsO}_4\text{-D}_2\text{O}$ SYSTEM

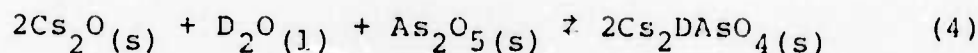
Cesium dideuterium arsenate is one stable crystalline phase in the ternary system  $\text{Cs}_2\text{O}(\text{s})\text{-As}_2\text{O}_5(\text{s})\text{-D}_2\text{O}(\text{l})$ . Figure 1 shows a projection of all important compounds in this system on the ternary composition axes. These data resulted from our study of the phase relationships during this program. Under isobaric conditions, temperature and two concentration parameters are the variables.  $\text{CD}^*\text{A}$  can be formed according to the following stoichiometric reaction:



Other reactions in this ternary system which would yield solid phases are:



and



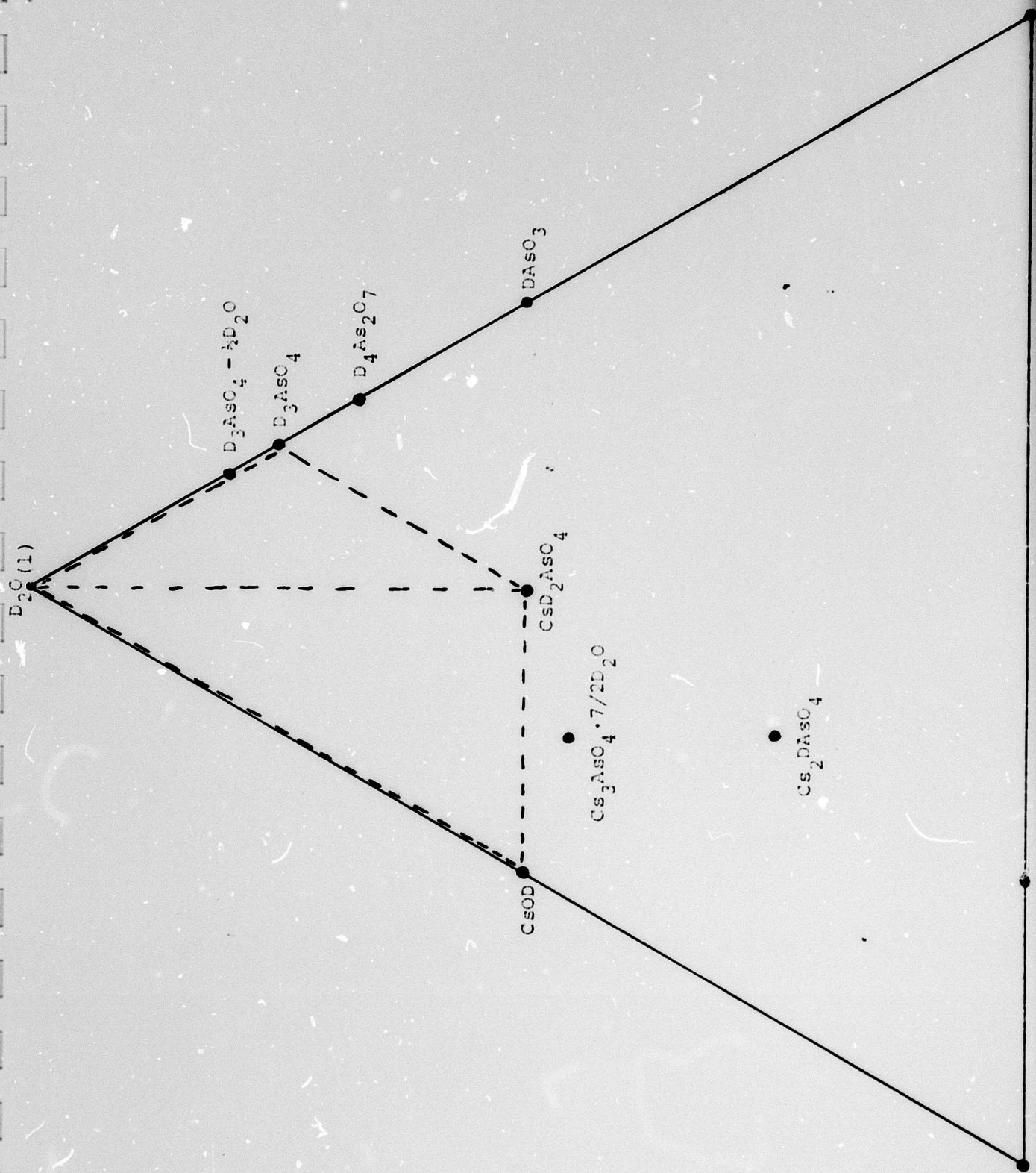
Therefore, since other compounds may possibly form, it is necessary to be relatively close to the correct stoichiometry in order to precipitate or grow from solution the desired crystalline phase.

The dashed lines in Figure 1 show the areas of particular interest for the growth of cesium dideuterium arsenate. These areas include the following two sub-ternary

**ISOMET**

Figure 1

The Ternary Systems  $\text{Cs}_2\text{O}(\text{s}) - \text{As}_2\text{O}_5(\text{s}) - \text{D}_2\text{O}(\text{l})$  [Mole %]



and binary systems:

- i)  $\text{CsD}_2\text{AsO}_4(\text{s}) - \text{D}_2\text{O}(\text{l}) - \text{D}_3\text{AsO}_4(\text{l})$
- ii)  $\text{CsD}_2\text{AsO}_4(\text{s}) - \text{D}_2\text{O}(\text{l}) - \text{CsOD}(\text{s})$
- iii)  $\text{CsD}_2\text{AsO}_4(\text{s}) - \text{D}_2\text{O}(\text{l})$

All these systems are of importance when an adjustment of  $P_{\text{H}}$  is necessary to enhance crystal growth along particular crystallographic directions or change the relative supersaturation of a solution in a certain range of temperatures.

### 3.1 Phase Stability of $\text{CsD}_2\text{AsO}_4$

Because of the possibility of second phase precipitation in the  $\text{CsD}_2\text{AsO}_4 - \text{D}_2\text{O}$  binary, the primary phase stability region of  $\text{CD}^*\text{A}$  had to be determined as a function of  $P_{\text{H}}$  and temperature.

The  $P_{\text{H}}$  of the solution was read by a Corning Digital 110  $P_{\text{H}}$  Meter at temperature. Harelco reference buffers were employed to calibrate the  $P_{\text{H}}$  meter. Powder diffraction patterns were taken of the precipitated crystalline material. Nickel filtered  $\text{CuK}\alpha$  radiation was used.  $\text{Al}_2\text{O}_3$  powder was employed as an external calibration standard. The data were taken at two degrees 20 per minute at a chart speed of 5 cm/min. Table 5 contains the data collected during this study.

Saturated solutions were prepared at various temperatures. These solutions were then cooled until a precipitate formed. The solution was then slowly heated and stirred until the precipitate dissolved and then the  $P_{\text{H}}$  measured. Then the solution was cooled

TABLE 5

Primary Phase Limits For CD\*A As A Function  
Of  $P_H$  And Temperature

<u><math>P_H</math> (+ 0.01)</u>	<u><math>T</math> (+ 1.0°C)</u>	<u>Phase(s) Precipitated</u>
9.00	60	CD*A
9.00	30	CD*A
9.00	10	CD*A
8.50	60	CD*A
8.50	20	CD*A
8.00	60	CD*A
8.00	30	CD*A
8.00	10	CD*A
7.50	60	CD*A
7.50	20	CD*A
7.00	60	CD*A
7.00	30	CD*A
7.00	10	CD*A
6.50	60	CD*A
6.50	20	CD*A
6.00	60	CD*A
6.00	30	CD*A
6.00	10	CD*A
5.50	60	CD*A
5.50	20	CD*A
5.00	60	CD*A
5.00	30	CD*A



TABLE 5 (CONTINUED)

$P_H (\pm 0.01)$	$T (\pm 1.0^\circ\text{C})$	Phase(s) Precipitated
5.00	10	CD*A
4.50	60	CD*A
4.50	20	CD*A
4.00	60	CD*A
4.00	30	CD*A
4.00	10	CD*A
3.50	60	CD*A
3.50	20	CD*A
3.00	60	CD*A
3.00	30	CD*A
3.00	10	CD*A
2.50	60	CD*A + Other Phase (X)
2.50	20	CD*A + Other Phase (X)
2.00	60	Other Phase (X)
2.00	30	Other Phase (X)
2.00	10	Other Phase (X)
1.50	60	Other Phases (X + Y)
1.50	20	Other Phases (X + Y)
1.00	60	Other Phase (Y)
1.00	30	Other Phase (Y)
1.00	10	Other Phase (Y)

slightly below this temperature and the solution decanted. The solid phase was dried in an oven at 65°C.

X-ray powder diffraction slides were prepared from portions of each precipitate. In this manner, the phase stability of CD\*A was mapped as a function of T and  $P_H$ . Cesium dideuterium arsenate was found to be the primary crystalline phase in the  $P_H$  range 3.00 to 9.00 in the temperature interval of 60 to 110°C. The two other crystalline phases (X and Y) listed in Table 5 did not compare to any published X-ray powder diffraction pattern<sup>5</sup> and could not be readily indexed. It was determined that these phases were two distinct compounds by the non-variance of the diffraction peaks with respect to 2 $\theta$  from pattern to pattern.

### 3.2 Solubility of $\text{CsD}_2\text{AsO}_4$ in $\text{D}_2\text{O}$

An important parameter in crystal growth from aqueous solutions is the change in solubility as a function of temperature,  $(\partial s / \partial T)_{n_i, P}$ , where  $s$  = solubility of CD\*A (g/100g solvent)

$T$  = temperature (°C)

$n_i$  = constant number of moles of solvent and other ionic species

$P$  = constant atmospheric pressure.

Growth runs are made in a region of nearly linear solubility ( $f(T)$ ) with  $(\partial s / \partial T)_{n_i, P}$  large enough to deposit a reasonable number of grams over a certain  $\Delta T$ .

To accurately determine the solubility curve (saturation concentration), the supersaturation variable must be eliminated.<sup>6-7</sup> This is done by preparing a nearly saturated solution at a particular temperature and then rapidly lowering the temperature until precipitation occurs. Then the solution plus precipitate are held at a fixed temperature and more solvent slowly added, via a calibrated buret, until all the solids dissolve.

The solution is constantly stirred during the determination. Figure 2 is a plot of the solubility of  $\text{CsD}_2\text{AsO}_4$  as a function of temperature. It is evident that this material forms a highly concentrated solution (19.1 molal at  $40^\circ\text{C}$ ). Figure 3 is a TX section of the  $\text{CsD}_2\text{AsO}_4 - \text{D}_2\text{O}$  binary in mole percent  $\text{D}_2\text{O}$ . This corresponds to a section of the projection in Figure 1 of this binary (dashed lines). Other data collected during the solubility determination were the change in  $P_{\text{H}}$  versus temperature of a CD\*A solution saturated at  $20^\circ\text{C}$ . The  $P_{\text{H}}$  value at  $20^\circ\text{C}$  represents the neutral  $P_{\text{H}}$  of a CD\*A aqueous solution. Figure 4 is a plot of these data. For an undersaturated CD\*A aqueous solution, the  $P_{\text{H}}$  increases as the temperature increases.

### 3.3 Specific Gravity and Kinematic Viscosities of CD\*A Solutions

These data were determined in order to better understand the growth process and growth difficulties of CD\*A from  $\text{D}_2\text{O}$ . Table 6 shows the change in density as a function of temperature of cesium dideuterium arsenate solutions saturated at two temperatures. Table 7 shows the change in the relative kinematic viscosity as a function of temperature of the same CD\*A aqueous solutions.

The solution densities were determined by the pycnometric method. In this particular determination, the accuracy of the measurement was  $\pm 0.001$  g/cc. For more accurate determinations (fourth or fifth place), the variation of the density of air due to changes in barometric pressure, room temperature and relative humidity must be considered. Distilled water served as the calibration liquid.



Solubility of CD\*A (g/100ml D<sub>2</sub>O)

Figure 2 - Solubility of CD\*A as a Function of Temperature

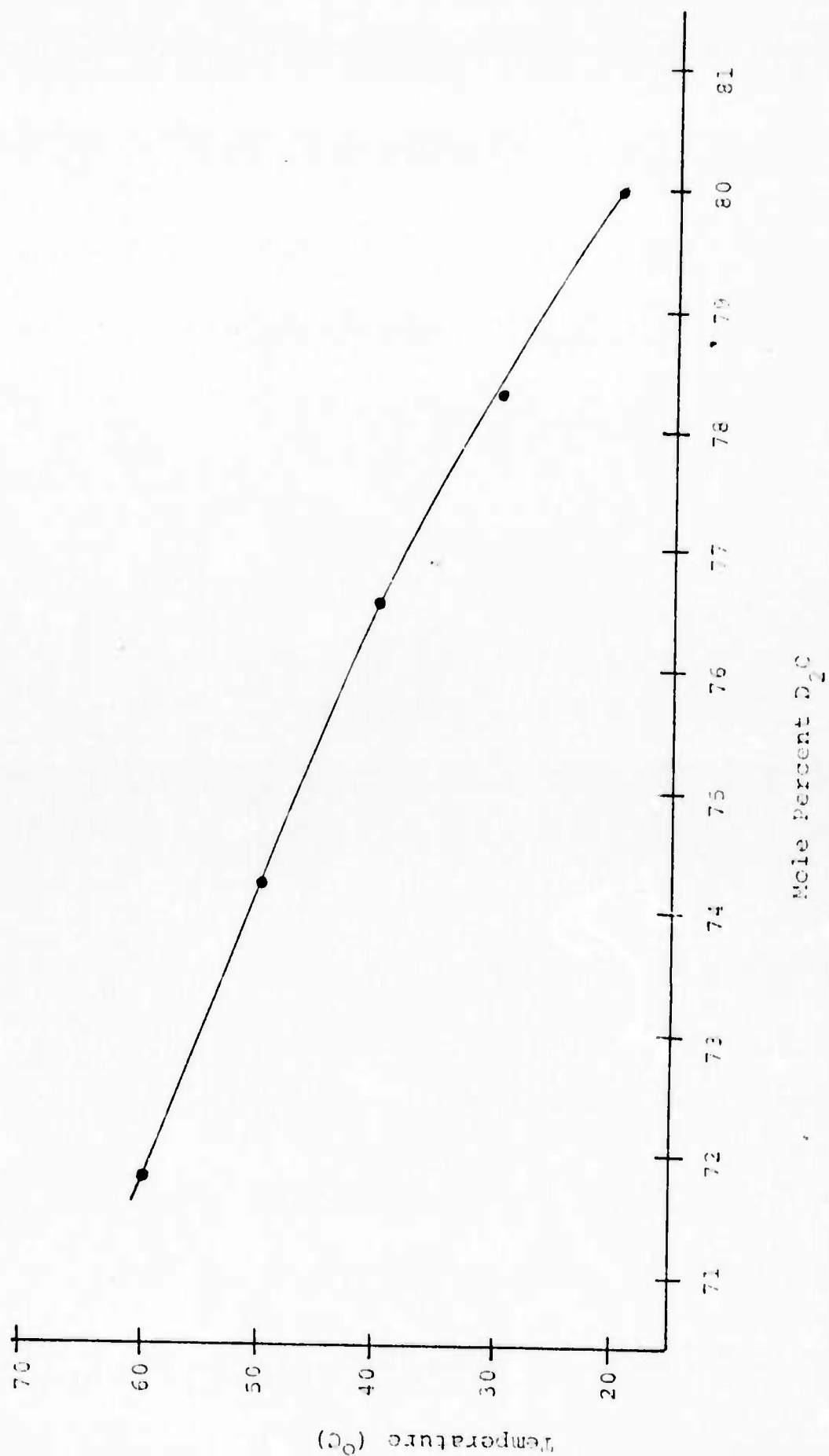


Figure 3 - TX Section of the CD-A- $D_2O$  Binary

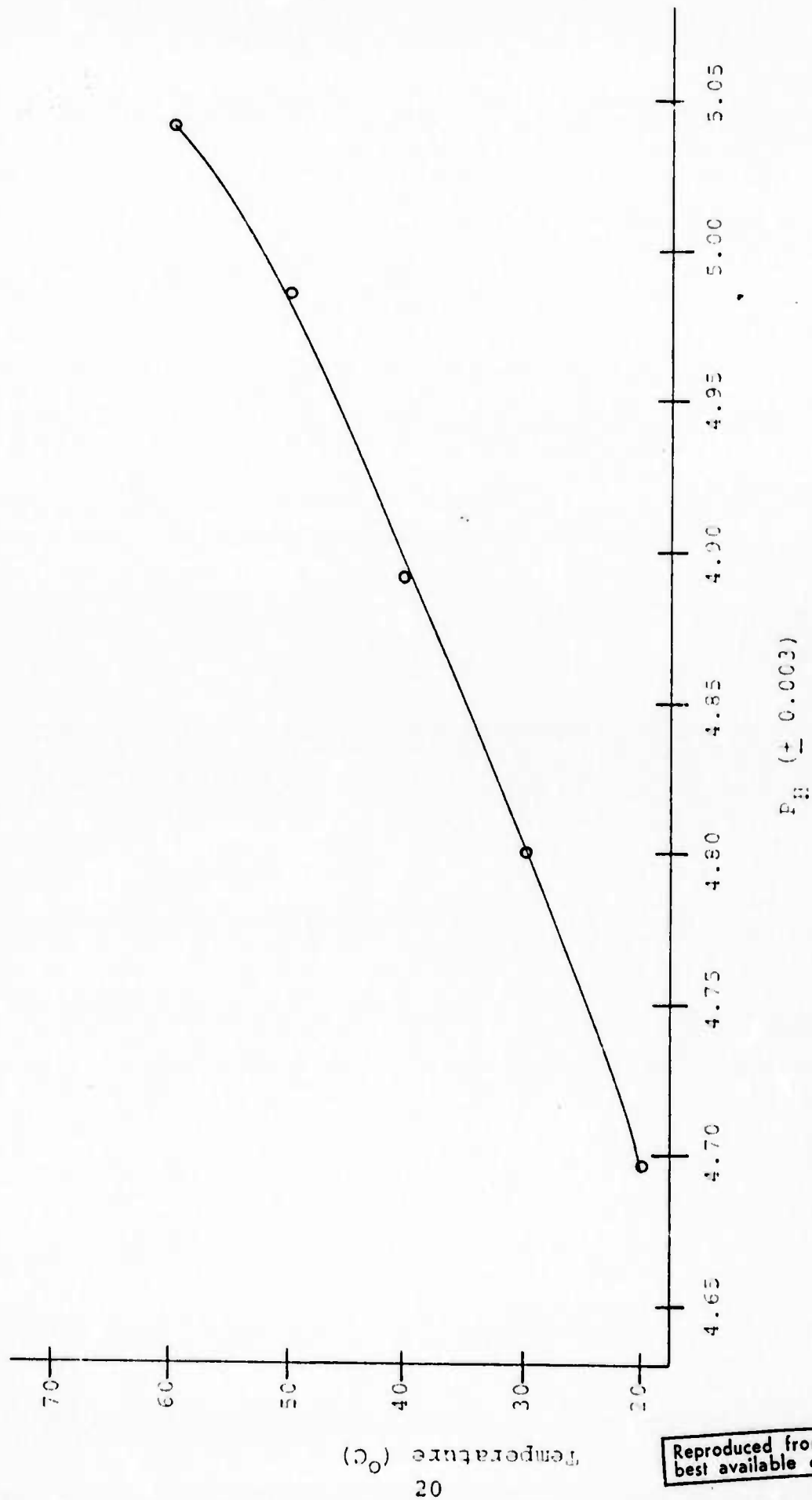


Figure 4 -  $pH$  Versus Temperature of a Saturated CD\* A Solution

TABLE 6Densities of  $\text{CsD}_2\text{AsO}_4$  Solutions As A Function of TemperatureSolution A ( $T_{\text{sat.}} = 20^\circ\text{C}$ )

<u><math>\rho(\text{g/cc})</math></u>	<u><math>T(^{\circ}\text{C})</math></u>
2.187	20
2.181	30
2.174	40
2.166	50
2.160	59

Solution B ( $T_{\text{sat.}} = 40^\circ\text{C}$ )

<u><math>\rho(\text{g/cc})</math></u>	<u><math>T(^{\circ}\text{C})</math></u>
2.466	59
2.462	65



TABLE 7.

Relative Kinematic Viscosities of  $\text{CsD}_2\text{AsO}_4$

Solutions As A Function Of Temperature

Solution A ( $T_{\text{sat.}} = 20^\circ\text{C}$ )

<u>v (centistokes)</u>	<u>T (<math>^\circ\text{C}</math>)</u>
1.0935	25
1.0900	28
0.9649	30
0.7542	40
0.6004	50
0.5045	59

Solution B ( $T_{\text{sat.}} = 40^\circ\text{C}$ )

<u>v (centistokes)</u>	<u>T (<math>^\circ\text{C}</math>)</u>
1.3824	50
1.1149	59

The kinematic viscosities were determined by Stoke's law which relates the viscosity of a liquid to the frictional force acting on a moving sphere. The tube constant was experimentally determined by measuring the time of fall through a liquid of known density and viscosity as a function of temperature. From these data, the relative kinematic viscosities can be calculated. The determination of absolute viscosities is difficult and is dependent upon very accurate measurements of the apparatus employed.

It is known that solutions of high viscosity can drastically slow down, and sometimes, eliminate concentration currents. Therefore, growth can occur only by means of diffusion. This also results in the inability of the growing surface to release the latent heat of crystallization. Under this condition, edge and corner growth as well as dendritic growth tends to occur."

### 3.4 Supersolubility Of $\text{CsD}_2\text{AsO}_4$ In $\text{D}_2\text{O}$

All solute-solvent systems possess some degree of supersaturation. Figure 5 illustrates the relative positions of the saturation and supersaturation curves. Many papers have been published which deal either with the experimental determination of the degree of supersaturation<sup>6-12</sup> or the thermodynamics involved.<sup>13-20</sup> These are, by far, an incomplete list and only serve to show the interest, as well as the importance of such data. It is known that the habit (morphology), size, and crystal quality are related to the degree of supersaturation of a solution.<sup>6-12</sup> The limiting supersaturation depends upon the

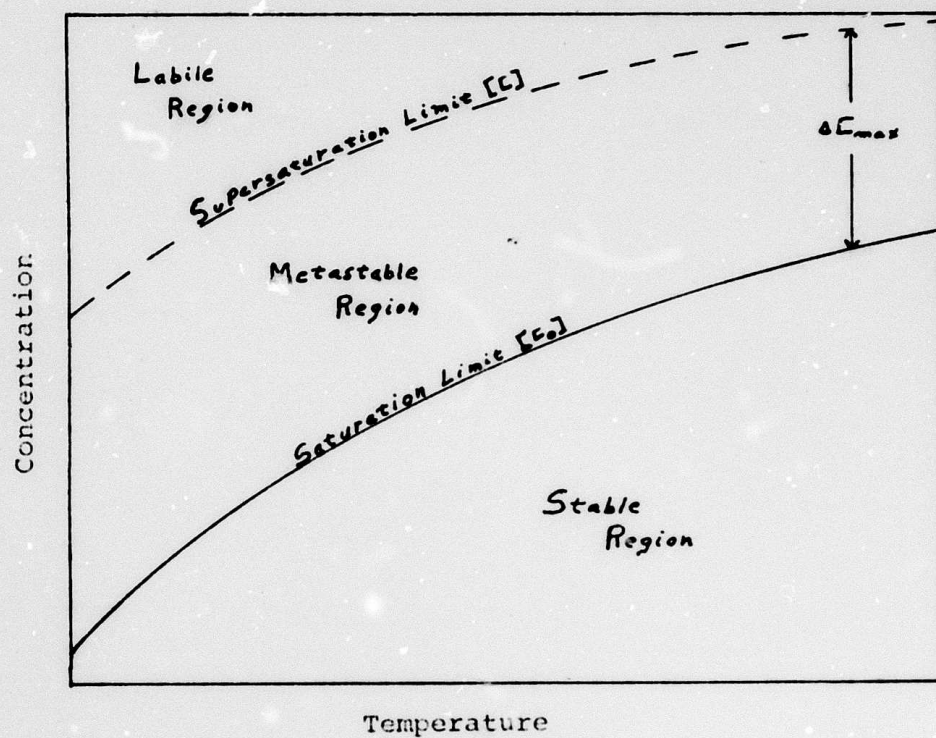


Figure 5 - Supersaturation and Saturation Relationship  
For Any Solute-Solvent System

nature of the solute and solvent, rate of rotation, temperature, rate of change of temperature, agitation,  $P_H$  of solution, and impurities.

The supersaturation of a particular solute-solvent can be calculated from the following equation:<sup>9</sup>

$$\Delta C_{\max.} = k_t F C_o = [C - C_o]_t \quad (5)$$

where

$\Delta C_{\max.}$   $\equiv$  limiting supersaturation (g salt/100 g solvent),

$F$   $\equiv$  formula weight of solute (g/mole),

$k_t$   $\equiv$  experimental constant,

$C_o$   $\equiv$  saturation concentration (g salt/100 g solvent),

$C$   $\equiv$  supersaturation concentration (g salt/100 g solvent),

$t$   $\equiv$  temperature ( $^{\circ}\text{C}$ ).

From this equation, coupled with the experimentally determined saturation concentrations (Figure 2), the limiting supersaturation and supersaturation can be calculated for the  $\text{CsD}_2\text{AsO}_4 - \text{D}_2\text{O}$  system (Table 8). Table 9 compares the supersaturation limit of CD\*A with a number of other inorganic salt solutions.<sup>6</sup> By far, CD\*A possesses the largest metastable region of all the salts listed.

It is known that when there are not sufficient moles of solvent available to form complete "solvation spheres" around all ions  $[\text{Cs}$  and  $\text{D}_2\text{AsO}_4]$  in solution,<sup>21-26</sup> the average strength of an ion-solvent bond increases. This also increases the polarity of the dipole formed, and therefore, the possibility of "secondary bonding" of this ion-solvent molecule with another

TABLE 8Supersaturation Data As A Function of TemperatureIn The  $\text{CsD}_2\text{AsO}_4 - \text{D}_2\text{O}$  System

<u>C (g/100g)</u>	<u>C<sub>o</sub> (g/100g)</u>	<u><math>\Delta C_{\text{max.}}</math> (g/100g)</u>	<u>t (°C)</u>
366.6	345.0	21.6	20
415.7	380.0	35.7	30
471.4	419.0	52.4	40
557.4	482.0	75.4	50
643.7	542.0	101.7	60

TABLE 9

$C_o$  and  $\Delta C_{\max.}$  of Various Salt Solutions at  $40^\circ\text{C}$

<u>Material</u>	<u><math>C_o</math> (g/100g)</u>	<u><math>\Delta C_{\max.}</math> (g/100g)</u>
$\text{NH}_4\text{NO}_3$	297	8.9
$\text{NaNO}_3$	104	3.6
$\text{KNO}_3$	63.9	3.2
$\text{Ba}(\text{NO}_3)_2$	14.2	1.1
$\text{NH}_4\text{Cl}$	45.8	1.2
$\text{NaCl}$	36.6	0.4
$\text{KCl}$	40.0	1.6
$\text{HgCl}_2$	10.2	1.4
$\text{NH}_4\text{H}_2\text{PO}_4$	56.6	4.2
$\text{KD}_2\text{PO}_4$	33.5	2.1
$\text{CsD}_2\text{AsO}_4$	419	52.4

## ISOMET

similar molecule increases. As a result, a highly associated solution results. Controlled crystallization is very difficult under these conditions.

The cesium cation usually has a primary coordination sphere of 8 to 12 in a solid (Cs Cl structure). One can reasonably assume the same coordination in an aqueous solution. From Figure 3, the ratio of moles of  $D_2O$ /mole of  $CD^*A$  is approximately 3:1. Therefore, one would suspect a highly "structured"  $CD^*A$  solution.



#### 4. THE $\text{CsD}_2\text{AsO}_4 - \text{D}_2\text{O} - \text{R(OD)}_n$ SYSTEMS

During the latter stages of this investigation, it became evident that reproducible growth from aqueous CD\*A solutions was, at best, difficult. Therefore, an initial search was made for an adequate binary solvent with the stipulation that the other solvent possess a wide range of miscibility with  $\text{D}_2\text{O}$ . The following binary solvent systems were explored:

- i) Acetone -  $\text{D}_2\text{O}$
- ii) Ethanol -  $\text{D}_2\text{O}$
- iii) Methanol -  $\text{D}_2\text{O}$
- iv) Glycol -  $\text{D}_2\text{O}$
- v) Dioxane -  $\text{D}_2\text{O}$ .

This range of binary solvents could be examined because of our ability to exchange all hydrogens, if it became necessary. The complete exchange of all hydrogens is a complex technique and is necessary when a solution is prepared at low hydrogen activities.

First, a series of precipitates were collected from CD\*A - organic solvent and CD\*A -  $\text{D}_2\text{O} - \text{R(OD)}_n$  mixtures at various temperatures and mole ratios. These precipitates were dried at  $65^\circ\text{C}$  and X-ray powder diffraction slides were prepared. X-ray powder diffraction patterns were taken to check the phase(s) present in the precipitate. From these data, only two solvent systems precipitated CD\*A: ii) and iv). Of these two, the

glycol -  $D_2O$  system was superior to the ethanol -  $D_2O$  system. The ethanol -  $D_2O$  solvent system tended to separate into two layers when the  $CsD_2AsO_4$  precipitated.

#### 4.1 The Phase Stability of $CsD_2AsO_4$

All the data reported here pertains to completely deuterated glycol. Only one concentration was partially investigated: 30% glycol - 70%  $D_2O$ . The primary phase stability region was determined as a function of  $P_H$  and temperature. All preparatory and measurement techniques employed were exactly the same as those discussed in Section 3.1.

Cesium dideuterium arsenate was found to be the primary crystalline phase in the  $P_H$  range of 4.00 to 6.00 in the temperature interval of 40 to 20°C. At present, no  $P_H$  or phase stability data were taken outside this range.

#### 4.2 Solubility of $CsD_2AsO_4$ in $D_2O$ - Glycol

Figure 6 is a plot of the saturation concentration of CD\*A as a function of temperature in the deuterated glycol -  $D_2O$  solvent. The dashed lines represent the possible extension of the  $(\partial s / \partial T)_{n_i, P}$  to higher and lower temperatures. More data need be collected at various temperatures and glycol -  $D_2O$  mole ratios to completely define this solvent system. However, what can be said is that the equilibrium concentration of CD\*A has been reduced by more than a factor of two, at any particular saturation temperature, when compared to the CD\*A -  $D_2O$  system (Table 8).

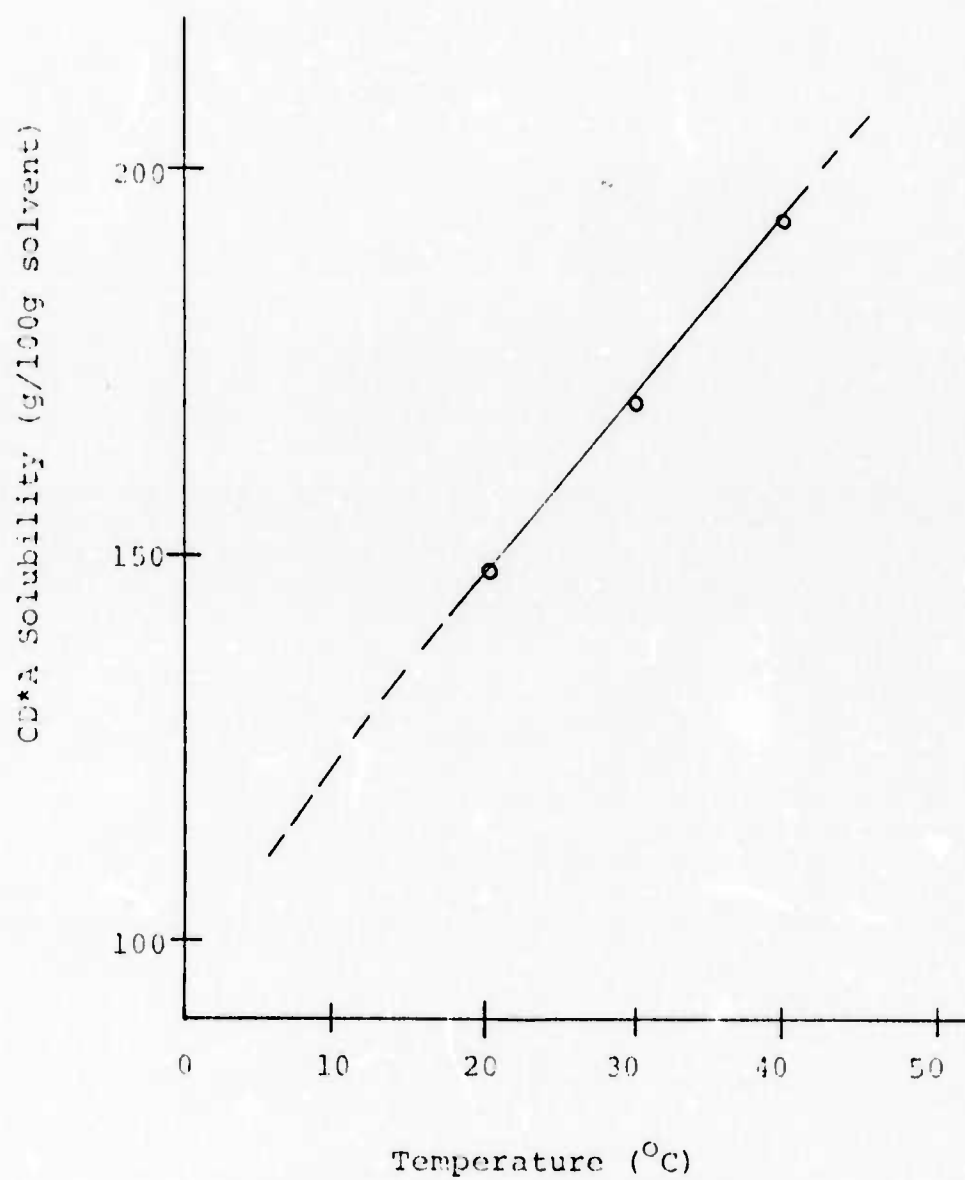


Figure 6 - Solubility of CD\*A in Glycol - D<sub>2</sub>O Solvent

#### 4.3 Supersolubility of $\text{CsD}_2\text{AsO}_4$ in $\text{D}_2\text{O}$ - Glycol

Equation (5) was employed for the calculation of the limiting supersaturation of CD\*A in this binary solvent system. Table 10 contains the data calculated from this equation.

Since the only difference is the  $C_o$ , the supersaturation concentration of CD\*A was reduced by more than a factor of two. This changed the ratio of solvent to solute from 3:1 to approximately 7:1 in the mixed solvent system. Further work on various mole ratios of deuterated glycol to  $\text{D}_2\text{O}$  could increase this to the desirable ratio of 15:1 (based upon our KD\*P data).

TABLE 10

Supersaturation Data As A Function Of Temperature  
In The  $\text{CsD}_2\text{AsO}_4 - \text{D}_2\text{O} - \text{Glycol}$  System

<u>C (g/100g)</u>	<u>C<sub>0</sub> (g/100g)</u>	<u><math>\Delta C_{\text{max.}}</math> (g/100g)</u>	<u>t (°C)</u>
157.3	148	9.3	20
185.9	170	15.9	30
218.3	194	24.3	40

## 5. THE GROWTH AND CHARACTERIZATION OF SINGLE CRYSTAL $\text{CsD}_2\text{AsO}_4$

Most of the growth runs were done in aqueous solutions. However, some growth data were collected in a mixed solvent system during the latter stages of this investigation. The following growth parameters were varied in these runs:

- i) Saturation temperature
- ii)  $P_H$  of solution
- iii) Deuteration level
- iv) Rate of rotation
- v) Seed orientation
- vi) Seed preparation techniques

The most suprising result was the effect of the seed preparation technique upon the growth perfection of  $\text{CD}^*\text{A}$  from aqueous solutions.

### 5.1 Seed Preparation

In all growth runs only Z-plates or caps were employed. The plates or caps were mounted either with the Z-direction in the vertical or horizontal plane. Usually one crystal was mounted with each orientation during a growth run for comparison.

Seed plates were prepared by the following procedure. First, a boule of  $\text{CD}^*\text{A}$  was oriented to within 2 minutes of arc with a two crystal X-ray spectrometer employing  $\text{CuK}\alpha$  radiation. After the  $a_0$  and  $c_0$  crystallographic axes are located and marked, the boule is then cut into plates with a string saw. The string-sawed surfaces of these plates were treated in different ways.

Some plates were water-polished on felt to remove the cut marks and others were water-polished with 300 to 600 grit

emory paper. Others were not touched at all after string-sawing. When seed caps were employed, no mechanical work was performed on the cap surface. The other end of the cap was string-sawed and finished by one of the above mentioned techniques.

In growth runs where no or a minimum amount of tapering occurred, no multiple twin growth resulted when perfect caps were employed. This was not the case when carefully prepared seed plates were used. A high degree of perfection was required for non-multiple growth in the high basic  $P_H$  range in aqueous solutions.

## 5.2 Aqueous Growth Data

A large number of growth runs were attempted in aqueous solutions. Table 11 contains a compilation of the critical run data. The data is listed according to  $P_H$  values. The run number gives the actual chronological order in which the runs were done.

The  $P_H$  of the solution was read by a Corning Digital 110  $P_H$  Meter usually 3 - 5°C above the determined saturation temperature. Reference buffers were employed to calibrate the  $P_H$  meter. The accuracy of the recorded  $P_H$  was  $\pm 0.002$  units. The saturation temperature of a solution was determined by suspending a seed of CD\*A in the solution and viewing the concentration currents emanating from the seed through a suitable optical system. The precision of this method is  $\pm 0.1^\circ\text{C}$ . Seed dimensions were measured with a vernier ( $\pm 0.05$  mm). A double pan balance was employed for weighing ( $\pm 0.02$ g) the



TABLE 11

## GROWTH DATA FROM AQUEOUS SOLUTION FUNG

Run #	P <sub>H</sub>	Vol. (L)	Sat. Temp. (°C)	Rot. Rate (rpm)	Seed dim. (ECR), Z (h) (mm.)	Seed dim. (EGR), Z (v) (mm.)	Seed dim. (AGR), Z (h) (mm.)	Seed dim. (AGR), Z (v) (mm.)	ΔT (°C)	Total grs. depos.	g/°C	Comments
39	3.62	1.5	29.5	6	19.8 x 22.4	27.9 x 28	19.1 x 20.1	94.5 x 56.5	2.2	210 +14 (x)	102	XtG Seeds diss.
42	3.73	1.5	35	14	N.A.	48 x 49	N.A.	N.D.	4.0	147	36.7	FG, MTW
36	4.94	1.15	37.7	10	23.2 x 25.2	29.5 x 29.5	23.5 x 24.2	29.3 x 26.8	5.3	99.3	18.9	T, FG
26	5.76	1.2	42	20	31.8 x 31.8	19.1 x 19.1	N.D.	N.D.	N.D.	N.D.	N.D.	T, FG
28	5.19	1.24	45.9	20	31.8 x 31.8	19.1 x 19.1	N.D.	N.D.	8.9	146.3	16.4	T, FG, SC
37	5.26	1.24	45	14	22.4 x 20.1	30.5 x 30.2	20.7 x 21.8	31.2 x 31.1	5.5	123.7	22.5	T, FG
41	5.23	1.5	50.5	14	15.5 x 16.5	18.3 x 18.4	15.6 x 15.8	19.8 x 17.5	1.5	39.8	26.5	50% D soln., T
29	6.54	1.5	56.9	20	27.8 x 25.6	24.5 x 25	N.D.	N.D.	2.2	86.8	39.5	T, FG
31	6.54	1.5	55.5	6	27.8 x 25.6	24.5 x 25	N.D.	N.D.	5.7	133.5	23.4	T, FG
33	6.47	1.5	31.5	6	24.5 x 27.4	24 x 25	23 x 26	24 x 25	10	91 +36 (x)	12.7	T, FG
35	6.49	1.25	31.5	20	19.2 x 21	32 x 32	19.5 x 20.9	29.8 x 30.6	6.3	95.9	15.3	T, FG
40	6.44	1.5	26.8	10	23.4 x 24.5	28.3 x 28.3	N.D.	N.D.	N.D.	N.D.	N.D.	XtG, T, MTW
27	7.76	.68	40.2	20	25.4 x 19.1	N.A.	N.D.	N.A.	10.5	120	11.4	FG, ST

TABLE 11 (CONTINUED)

Run #	P <sub>H</sub>	Vol. (L)	Sat. Temp. (°C)	Rot. Rate (rpm)	Seed dim. (BGR), Z(h) (mm)	Seed dim. (BGR), Z(v) (mm)	Seed dim. (AGR), Z(h) (mm)	Seed dim. (AGR), Z(v) (mm)	ΔT (°C)	Total grs. depos.	g/°C	g/L	Comments
38	8.20	1.25	31.3	6	18.1 x 19.1	31.5 x 31.2	19.8 x 21	37.2 x 35.7	7.5	97.7 +11(x)	14.4	86.6	FG, MTW, EG
44	8.23	1.2	38.8	20	18.8 x 18.3	28.6 x 28	22 x 22	32.5 x 33.5	7.9	84.3	10.7	70.3	FG, MTW, EG
45	8.50	3.8	39.6	20	37 x 35.5	30 x 30	38.5 x 37	32 x 32	4	N.D.	N.D.	N.D.	FG, MTW, EG
45-A	8.11	1.22	23.8	23	21 x 21	N.A.	27 x 26	N.A.	22.2	179.7 +74(x)	11.4	207.7	FG, MTW, EG
49	8.59	3.62	39.7	20	32 x 32	N.A.	38 x 36	N.A.	7	240.7	34.4	66.5	FG, MTW, EG
50	8.23	1.2	40.1	N.D.	11 x 21 9 x 24	N.A.	15 x 27 10 x 29	N.A.	18.2	90.1	5.0	75.1	FG, EG
55	8.00	1.5	50	6	25 x 26 25 x 26	N.A.	N.D.	N.A.	N.D.	N.D.	N.D.	N.D.	MTW, EG
43	9.05	1.4	39.2	15	21.8 x 21.8	25 x 25	22 x 21.2	N.D.	3.7	50	13.5	35.7	FG, MTW, EG

Abbreviations employed in Table 11

BGR ≡ before growth run  
 Z(h) ≡ Z direction in horizontal plane  
 Z(v) ≡ Z direction in vertical plane  
 AGR ≡ after growth run  
 (x) ≡ spurious nucleation  
 xtG ≡ extraneous growth  
 N.A. ≡ not applicable

N.D. ≡ no data  
 FG ≡ flawed growth  
 MTW ≡ multiple twinning  
 T ≡ tapering  
 GC ≡ green coloration  
 ST ≡ slight tapering  
 EG ≡ edge growth

seed plates prior to and after the growth runs.

The main growth problems encountered in aqueous solutions of  $\text{CsD}_2\text{AsO}_4$  were:

- i) continuous flawing (banding) of the crystal during growth,
- ii) tapering of the crystal along the  $c_0$  crystallographic axis,
- iii) preferential edge and corner growth on the seed,
- iv) multiple growth (growth twinning) of the seed plate or cap,
- v) irregular changes in  $(\partial s / \partial T)_{n_i, p}$ .

It can be seen from the data presented in Table 11 that the flawing encountered during growth in aqueous solutions occurred over the entire  $P_H$  range investigated. However, Run 41, carried out in a 50 mole % D solution, exhibited tapered growth with a minimal amount of flawing. Whether the flawing encountered is partially due to the deuteration level of the solution is still uncertain. More growth runs at various deuteration levels would have to be made. Figure 7 illustrates the flawing typically encountered at  $P_H$  values  $\geq 8$ . In this growth run the rotation rate was 20 rpm; the saturation temperature  $51^\circ\text{C}$ . The temperature drive,  $(dT/dt)$ , was constant during the entire run. A seed plate was employed.

In the  $P_H$  range of 4.5 to 7.5, tapering and flawing occurred in all runs in which the deuteration level was greater than 50%. Figures 8 and 9 illustrate the typical resultant growth in this  $P_H$  range. In this particular run seed plates

**ISOMET**

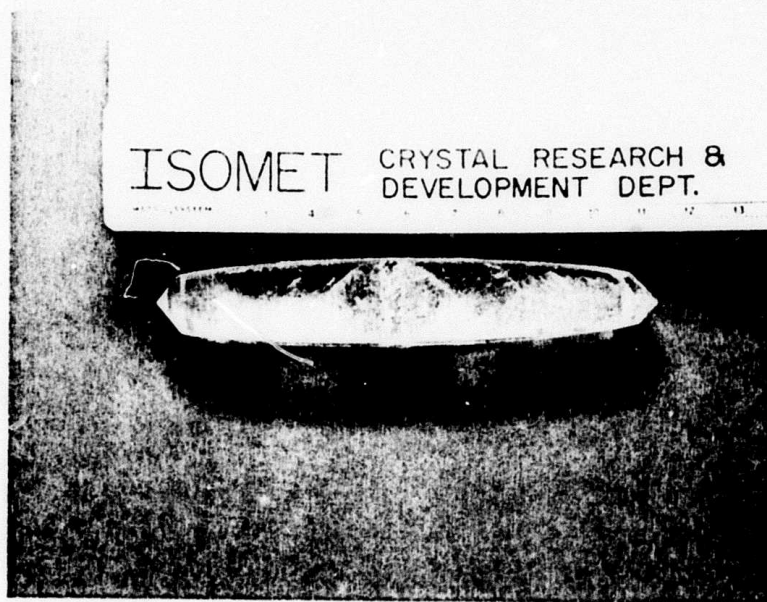


Figure 7 - Typical Growth From Seed

Plate at  $P_H$  Values  $\geq 8$

(scale in cm)

**ISOMET**

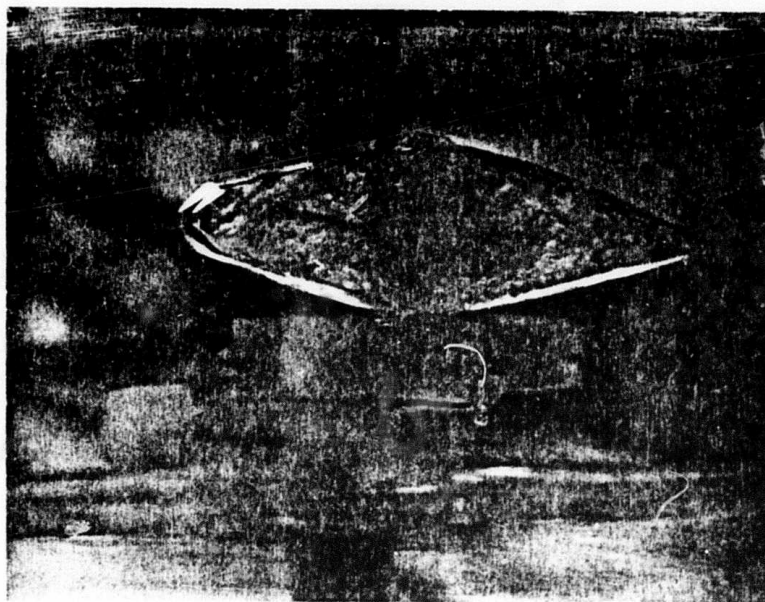


Figure 8 - Typical Growth Obtained With  
the Z Direction in the Horizontal Plane in the  
 $P_H$  Range 4.5 to 7.5. (Run 33)



Figure 9 - Typical Growth Obtained With the  
Z Direction in the Vertical Plane in the  
 $P_{II}$  Range 4.5 to 7.5. (Run 33)

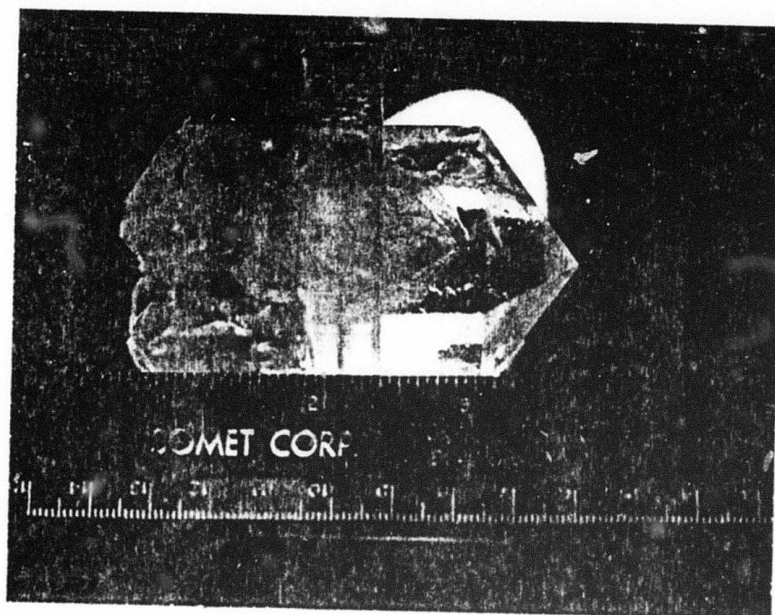
were used. Only near the tip of each boule is there clear growth. However, due to the tapering, the amount of useable material is drastically reduced.

It should be noted that in growth runs in which tapering occurred, little or no multiple growth was present. Edge and corner growth was also minimal. The degree of tapering can be minimized by adjusting the  $P_H$  of the solution to values  $\geq 8$ . However, when growth runs were done in this  $P_H$  range, XY growth increased by a large factor (Table 11). During the course of this investigation, we were able to increase the cross sectional area of the seeds by more than a factor of two in the high  $P_H$  range. We feel that further XY enlargement is quite possible by this technique. However, both good XY and Z growth cannot be accomplished under the same conditions of  $P_H$  and saturation temperature. In this  $P_H$  range, edge-corner and multiple growth greatly increased in the Z direction. These particular growth problems were never eliminated even when highly perfect caps were employed as seeds.

Figure 10 is a photograph of a boule grown from a highly basic aqueous solution. For this run, one side of the seed was a highly perfect cap which was not treated in any manner. The other side of the seed was a plate which was only string-sawed. Some flawing is evident on the cap end of the boule, as well as some multiple growth (beneath lower prism face in photograph). The seed plate end of the boule shows a high degree of flawing, multiple, edge and corner growth.



**ISOMET**




Reproduced from  
best available copy. 

Figure 10 - Photograph of As-Grown Boule From Run 49

(lower scale in cm)

For the purpose of comparison, growth runs were done duplicating the patented growth process of Adhav.<sup>27</sup> Run 55 in Table 11 is one such run made. Figure 11 is a photograph of a typical crystal grown by this process. In this particular run, each seed employed had one cap and plate end. Each surface was prepared in the same manner as described in the preceding paragraph. As can be seen, edge and corner growth occurred quite readily while the interior area of the cap partially dissolved. Results were the same when a spider holder was employed. We found that the growth problems were the same in this patented process and therefore, no particular advantage was gained by the addition of sodium tetraborate to the solution. In fact, the amount of edge and corner growth were much greater in these runs on seeds mounted with the Z direction in the horizontal plane.

Another approach that was employed in an attempt to produce reproducible, high quality CD\*A was the growth from large seed plates of ADP, AD\*P, KDP and KD\*P. These aqueous epitaxy experiments resulted in CD\*A needle growth from these plates (Figure 12). The lattice mismatch was far too great for this process to work. It should also be mentioned that growth by solvent evaporation resulted in the same growth problems as temperature lowering.

The final growth problem encountered in these aqueous solutions was the erratic changes in solubility as a function of temperature. In Run 39, the seed plates completely dissolved and a large platelet grew in the center of the rotator. An X-ray

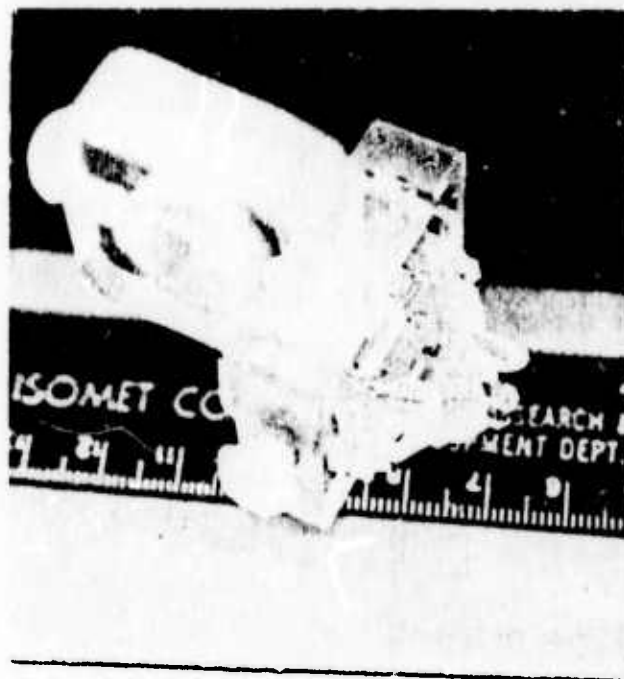


Figure 11 - Typical Growth Result From Aqueous  
Solution Doped With Sodium Tetraborate. (Run 55)

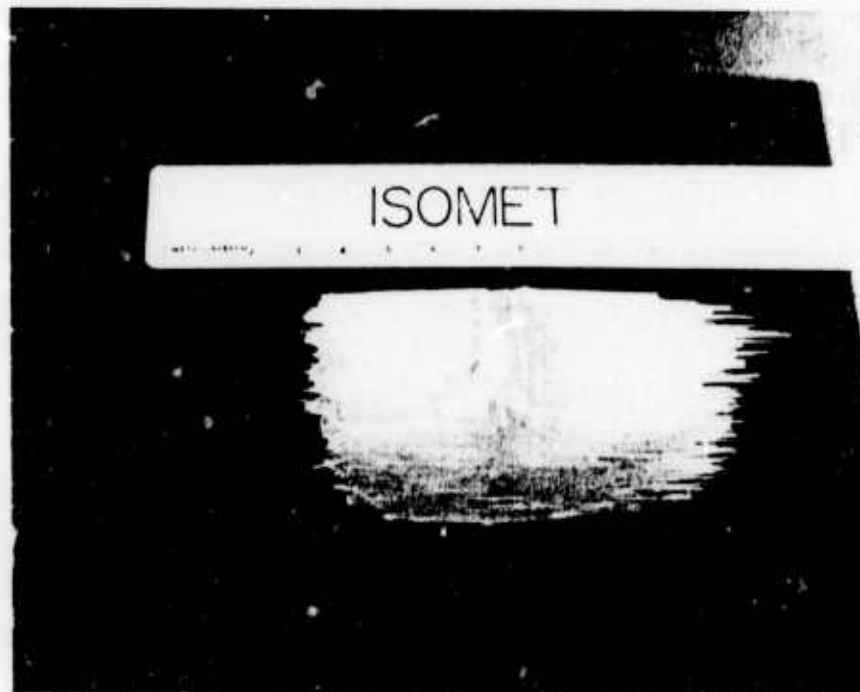


Figure 12 - Resultant Growth by Aqueous Epitaxy

diffraction analysis showed that this platelet was indeed CD\*A. Therefore, during the run, CD\*A dissolved in one part of the rotator and nucleated and grew in another part. A run was made utilizing this large plate as a seed (Run 42). The growth on this seed was highly irregular with a large number of grain boundaries evident. Another run which revealed the instability of the aqueous solution growth of CD\*A was Run 50. In this run caps were employed. As the run progressed the seeds began to grow quite well. When the temperature reached 38°C (2°C below saturation temperature), the new growth began to dissolve. Approximately a degree later, they began to grow again. This type of behavior further strengthened our belief that aqueous solution growth of CD\*A was too erratic to be controllable.

### 5.3 Mixed Solvent Growth Data

Because of the growth difficulties encountered in aqueous solutions, another solvent system was investigated. The solvent system which showed the most promise was a binary mixture of D<sub>2</sub>O and deuterated glycol.

Before a growth run was attempted in this solvent system, a number of static runs were done to roughly evaluate the best growth conditions of CsD<sub>2</sub>AsO<sub>4</sub> in this binary solvent system.

A static run consisted of a seed of CD\*A suspended in a certain mole ratio of solvent saturated at a particular temperature. No mechanical rotation or stirring was employed. Growth was accomplished by diffusion dependent upon whatever

thermal convection currents existed during the run. In all these static runs, the saturation temperature was  $43 \pm 0.5^{\circ}\text{C}$ . The solvent system was evaluated at 30, 50, 70% deuterated glycol. Under these limited conditions, the 30% deuterated glycol - 70%  $\text{D}_2\text{O}$  solvent mixture yielded the best growth. The solution  $P_{\text{H}}$  was  $4.70 \pm 0.01$ .

Further static runs were then done using this particular solvent ratio. In each static run the saturation temperature was  $42 \pm 0.5^{\circ}\text{C}$  and the  $P_{\text{H}}$  of the solution was varied from 4.0 to  $6.0 \pm 0.01$  units. Under these conditions, the best growth was obtained at  $P_{\text{H}}$   $5.51 \pm 0.01$ . At this point a typical growth run was made.

The seeds employed for this run were caps at one end and plates at the other. The rotation rate (reversible) was 10 rpm and the saturation temperature  $43.6 \pm 0.1^{\circ}\text{C}$ .  $P_{\text{H}}$  of the solution was adjusted to  $5.61 \pm 0.01$ . Figure 13 is a photograph of the resultant growth (in situ).

It can be seen that no flawing is evident from the cap end of the seed even though the  $P_{\text{H}}$  is quite low (compare to Figures 8 and 9). Some flawing is evident from the plate end of the seed. However, the amount of flawing is minimal when compared to that experienced in the aqueous growth runs. Also multiple growth and irregular changes in  $(\partial s / \partial T)_{n_i, P}$  have been eliminated in this growth run. The one growth problem yet to be eliminated is the degree of tapering. A run is now in progress in an attempt to reduce the tapering during growth.



Figure 13 - Photograph in situ of CD\*A growth  
in 30% deuterated glycol solution (Run 51).



In static runs it appears that the tapering can be controlled by the adjustment of the  $P_H$  of the solution. Much more data need be taken to verify this conclusion. However, these preliminary data show this system to be very promising for the reproducible growth of high optical quality CD\*A.

#### 5.4 The Actual Deuteration Level in $\text{Cs}(\text{D}_{1-x}\text{H}_x)_2\text{AsO}_4$ Crystals

In this particular crystal, and its homologs, the degree of deuteration can be calculated from the change in the ferroelectric transition temperature.<sup>28-29</sup> However, little effort has been devoted to the determination of the actual deuteration level in these crystals in the past. The common practice has been to quote the concentration of D in the crystal on the basis of the relative amounts of  $\text{D}_2\text{O}$  and  $\text{H}_2\text{O}$  in the growth solutions. It has been shown that the ferroelectric transition temperature has a linear dependence with respect to the deuteration level in this type of crystal.<sup>30</sup> Since there is an effective distribution coefficient of deuterium ions between the growth solution and the crystal, the deuterium level in the crystal must be measured. A reproducible technique has been developed at Isomet for this critical measurement.<sup>30</sup>

The ferroelectric transition temperature,  $T_C$ , of  $\text{CsH}_2\text{AsO}_4$  has been reported by a number of authors.<sup>28, 31-34</sup> Some of these authors also report values of  $T_C$  for  $\text{CsD}_2\text{AsO}_4$ .<sup>31, 33-34</sup> Table 12 is a compilation of these data. It should be noted that various methods were employed for these reported determinations.

TABLE 12

Reported Values of  $T_C$  For  $\text{CsH}_2\text{AsO}_4$  And  $\text{CsD}_2\text{AsO}_4$

<u>Material</u>	<u><math>T_C</math> (K)</u>	<u>Reference</u>
$\text{CsH}_2\text{AsO}_4$	140.3°	28
	143.3°	31
	145.0°	32
	143.3°	33
	145.4°	34
$\text{CsD}_2\text{AsO}_4$	212.0°	31
	212.4°	33
	190.2°	34

Also, the crystal quality would have an effect upon the absolute value of  $T_c$ . One would expect a spread of  $\pm 3K$  among reported values.

What is of main interest here is the large range of values of  $T_c$  reported for  $CsD_2AsO_4$ . One would immediately suspect that the deuteration level in Strukov's et. al. material was quite low compared to the other material. To verify this, the deuteration level of a crystal sample from Run 49 was determined by a spectrometric technique.<sup>30</sup> The deuteration level in the crystal was found to be  $85.62 \pm 0.05$  mole % D. The deuteration level of the growth solution was  $92.99 \pm 0.05$  mole % D. Next, differential thermal analyses were obtained on three separate crystalline samples from Run 49.  $T_c$  was found to be  $227^\circ \pm 1^\circ K$ . This value for  $T_c$  corresponds to a higher deuteration level than previously reported.<sup>31, 33-34</sup>

It is obvious from these data that the crystal  $Cs(D_{1.0}H_{0.0})_2AsO_4$  has yet to be grown. The highest deuteration level measured on  $Cs(D_{1-x}H_x)_2AsO_4$  was found in this study to be  $85.62 \pm .05$  mole percent.

From these data, a number of questions arise concerning the use of CD\*A as a second harmonic generator at  $1.06 \mu m$ . First, does the deuteration level of a crystal affect its intrinsic absorption at  $1.06 \mu m$ ? Secondly, what effect does the deuteration level have on the conversion efficiency of CD\*A? These questions can only be answered by measuring the SHG efficiency of various

CD\*A crystals of known deuteration levels. It is further hoped through this investigation that some definitive parameters could be found that govern SHG applications in this spectral region.

### 5.5 Optical Transmission

The optical transmission of a typical CD\*A crystal grown from pure D<sub>2</sub>O is illustrated in Figure 14. A deuteration level of 85.6% was measured for this sample. The sample had a path length of 10 mm along the Z axis and was polished flat to  $\lambda/5$  and parallel to 15 seconds. The transmission data was recorded on a Cary 14 Spectrometer. Absorption at 1.06  $\mu$  was estimated to be less than 1%. Refractive index data were not available and these measurements are now in progress.

### 5.6 Thermal Stability of CD\*A

A large number of CD\*A samples from various growth runs were examined by Differential Thermal Analysis (D.T.A.) to ascertain the ferroelectric transition temperature and thermal stability of this compound. The method and apparatus have been previously described.<sup>28, 29, 30</sup>

The relationship between deuteration level in the crystal and the ferroelectric transition temperature ( $T_c$ ) could not be completely defined. This was due to the lack of sufficient crystalline material required for the preparation of samples used in the %D determination. In KD\*P, typically 250 to 300g of crystalline sample are decomposed.<sup>30</sup> The actual deuteration level was determined only for Run 49 (Section 5.4). Table 13 lists the ferroelectric transition data obtained. While the

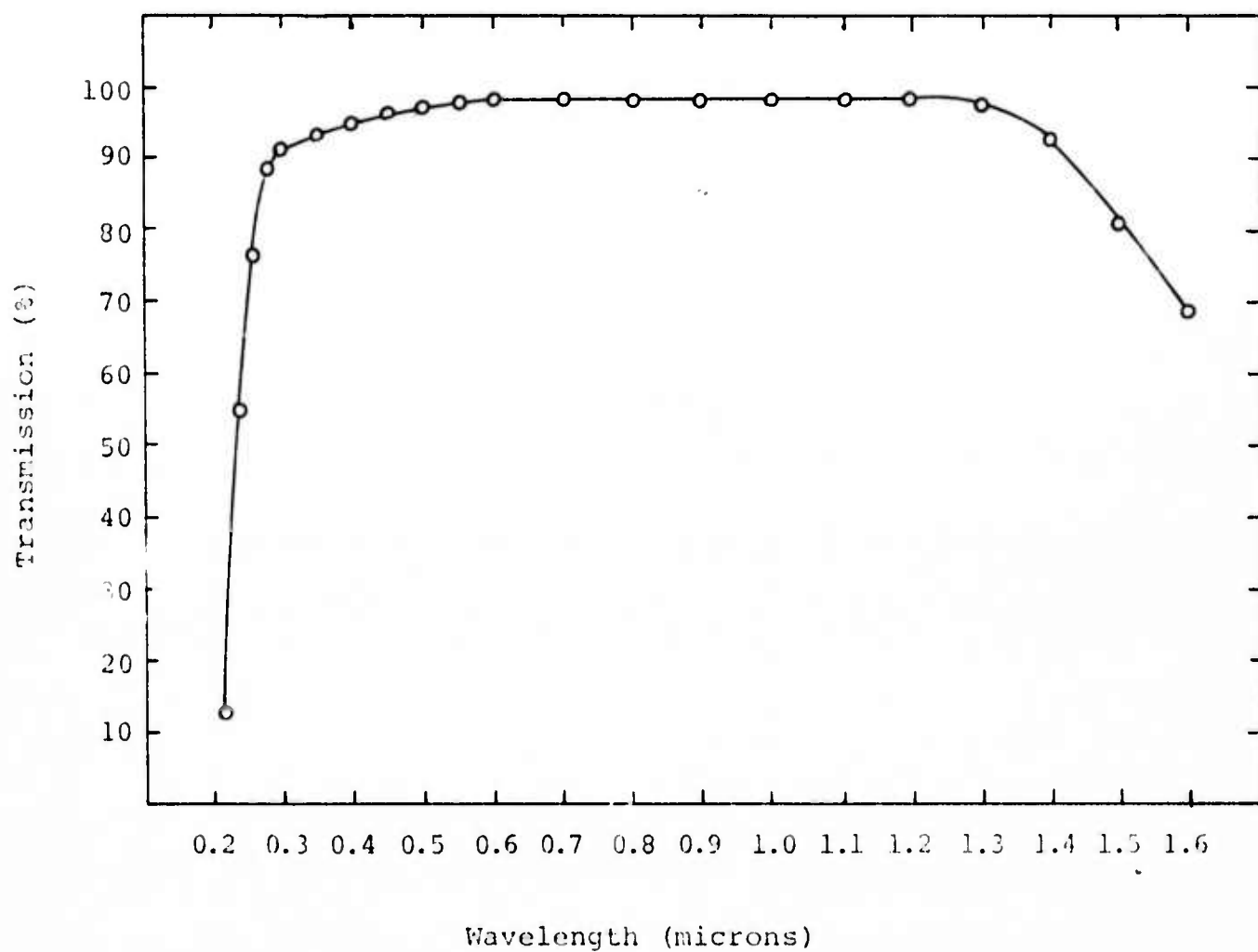


Figure 14 - Optical transmission of polished CD\*A crystal  
from Run 49 (corrected for Fresnel losses).

TABLE 13Comparison of  $T_c$  Data of  $\text{CsD}_2\text{AsO}_4$ 

<u>Sample</u>	<u><math>T_c</math> (K)</u>	<u>Reference</u>
	190 <sup>o</sup>	34
	212.0 <sup>o</sup>	31
	212.4 <sup>o</sup>	32
3/49 <sup>H</sup>	227.4 <sup>o</sup>	present work
9/48* <sup>H</sup>	225.7 <sup>o</sup>	present work
9/13 <sup>H</sup>	207.7 <sup>o</sup>	present work
9/21 <sup>H</sup>	209.6 <sup>o</sup>	present work

\* 85.6%D in crystal.

<sup>H</sup> All crystals grown from pure  $\text{D}_2\text{O}$ .

referenced data make various estimations of the deuteration level in the crystals measured, it is apparent that the only valid data point is 9/48 where both the deuteration level and the  $T_c$  were measured.

Values for the heat of transition for  $T_c$  were found to be sensitive to the crystals' deuteration level and were estimated to be 1.5 Kcal/mole for the highest deuteration level measured.

The examination of the high temperature stability and decomposition temperature of CD\*A resulted in the discovery of a phase transition previously unreported. The transition could not be investigated during the time remaining under the present contract. Decomposition of CD\*A was not observed up to 225°C.

Anomalous behavior of  $T_c$  was also observed when samples were subjected to mechanical grinding. It appears that when a sample is finely ground the ferroelectric transition disappears and is not detectable with our instrument. The cause of this behavior may shed some light into the ferroelectric mechanisms involved in the tetragonal arsenates. This behavior was not observed in similarly treated KD\*P.



## 6. CONCLUSIONS

From the systematic investigation carried out under this contract, the following accomplishments were made:

- i) The successful growth of CD\*A in both the aqueous and mixed solvent systems.
- ii) The growth of large cross section CD\*A in aqueous solution at high basic  $P_H$ .
- iii) The determination of the phase stability of CD\*A as a function of temperature,  $P_H$  and solvent.
- iv) The solubility of CD\*A as a function of temperature and  $P_H$ .
- v) The calculation of the degree of supersaturation of CD\*A as a function of temperature and solvent.
- vi) The determination of the growth problems of CD\*A in aqueous solutions and their relationship to the non-reproducible growth.
- vii) The elimination of most of the growth problems encountered in aqueous solutions by employing a mixed solvent.
- viii) The determination of the optical transmission of CD\*A single crystals grown from aqueous solutions.
- ix) The measurement of the actual deuteration level in single crystal CD\*A grown from an aqueous solution.
- x) The determination of ferroelectric and non-ferroelectric transitions in single crystal CD\*A as a function of temperature.

- xi) The determination of the lattice constants of a typical CD\*A crystal by a precise X-ray powder diffraction technique.

7. RECOMMENDATIONS

Based upon the wide spectrum of data collected and tabulated on the growth and solution chemistry of cesium dideuterium arsenate, the following areas of development and/or research are strongly suggested:

- i) The growth and characterization of cesium dideuterium arsenate produced under various growth conditions utilizing the mixed solvent system.
- ii) A complete comparison between the CD\*A single crystals grown from both the aqueous and mixed solvent systems.
- iii) Determination of the factors affecting the intrinsic absorption of CD\*A at  $1.06 \mu\text{m}$  and their relationships to the doubling efficiency and input power.

Although the initial growth runs in the mixed solvent system are very encouraging, more data need be taken at various mole ratios of  $\text{D}_2\text{O}/\text{D}$  glycol to find the optimum growth conditions. These data would, of necessity, have to include the phase stability, saturation and supersaturation concentrations of CD\*A in various mole ratios of solvents as a function of  $P_H$  and  $T$ .

Once the best growth conditions are found, a comparison ought to be made between the CD\*A grown from both solvents. This comparison should include the level of deuteration in the crystals, the purity and the doubling efficiencies. Coupled with this, a study should be made on what effect the deuteration level in the crystal has on the doubling efficiency. This would be related through the intrinsic absorption.

Certainly, this type of materials' characterization would be well worth the investment from both the theoretical and practical points of view.

8. REFERENCES

1. J.H. Boyden, E.G. Erickson, J.E. Murray and R. Webb, "Second Harmonic Generation", Final Technical Report (ONR), Contract No. N00014-71-C-0044, (1971).
2. A. Ferrari, M. Nardelli and M. Cingi, Cazz. Chim. Ital., 86, p. 1174, (1956).
3. G. Shklovskaya and Arkhipov, Russ. J. Inorg. Chem., 12, p. 1234, (1967).
4. R.W.G. Wyckoff, "Crystal Structures", Interscience Pub., N.Y., 3, p. 160, (1965).
5. JCPDS File, Inorg. Index, (1972).
6. H.E. Buckley, "Crystal Growth", John Wiley & Sons, N.Y., p. 1, (1961).
7. J.W. Mullin, "Crystallisation", Butterworth and Co., London, Chp. 2, (1972).
8. J.W. Mullin, A. Amatavivadhana and M. Chakraborty, J. App. Chem., 20, P. 153, (1970).
9. J. Synowiec, Kristall und Technik, 8, p. 701, (1973).
10. J.W. Mullin and A. Amatavivadhana, J. App. Chem., 17, p. 151, (1967).
11. Z. Salc and O. Soehnel, Kristall und Technik, 8, P. 811, (1973).

12. T. Blickle and S. Halcsz, Kristall und Technik, 8, p. 679, (1973).
13. R. Ghez, J. Cryst. Growth, 19, p. 153, (1973).
14. B. Lewis, J. Cryst. Growth, 21, p. 29, (1974).
15. A.R. Konak, J. Cryst. Growth, 19, p. 247, (1973).
16. E.V. Khamiskij, Kristall und Technik, 8, p. 107, (1973).
17. G.K. Kirov, J. Cryst. Growth, 20, p. 171, (1973).
18. J.H. Magill and H.M. Li, J. Cryst. Growth, 19, p. 361, (1973).
19. T. Nakai and K. Miyake, Mem. Fac. Eng., Hiroshima Univ., 5 (1) p. 1, (1973).
20. W.A. Tillier and C. Kang, J. Cryst. Growth, 2, p. 345, (1968).
21. D.R. Rosseinsky, Chem. Rev., 65, p. 467, (1965).
22. J.E. Desnoyers and C. Jolicœur, "Modern Aspects of Electrochemistry," Plenum Press, N.Y., Chp. 1, (1967).
23. A.J. Parker, "Advances in Physical Organic Chemistry", Academic Press, N.Y., Chp. 1, (1967).
24. R. Alexander, E. Ko, A.J. Parker and T. Broxton, J. Am. Chem. Soc., 90, p. 5049, (1968).
25. W.E. Morf and W. Simon, Helv. Chim. Acta, 54, p. 151, (1971).

26. U. Mayer and V. Gutmann, Structure and Bonding, 12, p. 113, (1972).
27. R.S. Adhav, "Cesium Dideuterium Arsenate Crystallization Process and Solution," Patent No. 3,748,102, 24 July, (1973).
28. G.M. Loiacono, Mat. Res. Bull., 5, p. 775, (1970).
29. G.M. Loiacono, Ferroelectrics, 5, p. 100, (1973).
30. G.M. Loiacono, J.F. Ealascio and W. Osborne, App. Phys. Letters, 24, #10, (1974).
31. C.C. Stephensen, J.M. Corbella and L.A. Russell, J. Chem. Phys., 21, p. 1110, (1953).
32. J. LeBot, S. LeMontagner and Y. Allain, Compt. Rend., 236, p. 1409, (1953).
33. A.R. Ubbelohde, "Melting and Crystal Structure", Clarendon Press, Oxford, England, (1965).
34. B.A. Strukov, A. Baddur, V.I. Zinenko, V.K. Mikhailov and V.A. Koptsik, Sov. Phys. Sol. St., 15, p. 1347, (1974).